Study on Characteristics of Weld Defect and its Prevention in Electron Beam Welding (Report Ⅳ)†
——Relationship between Weld Defect and its Formation Phenomenon——

Yoshiaki ARATA,* Kiyoshi TERAI** and Shozo MATSUDA**

Abstract

By the results obtained from penetrating phenomenon observed by X-ray occurred from the beam holes during electron beam welding, strong and weak waves of beam flow generated in beam holes occurred periodically, and this phenomenon was proved to be completely in accordance with spiking phenomenon.

The solidification pattern formed by segregation when welding condition was changed using insert metal was observed. From the results obtained from the abovementioned observation, it was proved that in welding in beam active zone with iron-based alloy, irregularity points are easily formed in molten pool, and also voids are easily formed at the abovementioned part.

Following the observation results of such weld phenomenon, we concluded that this behavior of fluidity in molten pool and the movement of beam flow are closely related and also defect is formed by the interaction between these two.

1. Introduction

On rare occasions, typical types of weld defects occur in electron beam weld metal. We have already reported about occurring characteristics and metallurgical features of weld defects[1)2)3)]. It has been proved that many of these defects depend upon beam characteristics like beam output or beam active zone and solidification process or alloying element correlated to welding condition like active beam parameter a_b.

Generally in electron beam, beam hole is formed by drilling accompanied by strong vaporization phenomenon caused by momentary melting or boiling on irradiation face. Beam hole which is formed so quickly that any practical thermal conductivity phenomenon can't be accompanied is called "Dry beam hole". On the contrary, beam hole whose circumference is heated and molten with enough thermal conductivity and also whose moving zone is filled with its molten metal is called "Wet beam hole".[4)] It is considered that such welding phenomenon has close relationship to weld defect. But no detail study has been made yet concerning this relationship between them.

We conducted the inquiry on characteristics of concentration distribution of X-ray amount occurring from beam hole during welding[5)], and also observed solidification pattern in case of changing welding conditions using insert metal. Then we studied on the relationship between morphology of weld defect and behavior of molten metal.

2. Experimental Procedure

2.1 Materials used and welding method

The materials used in this experiment are three types of iron-based alloys such as SUS304, SUS304N containing 0.2% nitrogen and SM41, and also two types of alminium alloys such as pure alminium 1200, and 5083 alloy containing 4.5% Mg. The chemical composition of these materials used are equivalent to the ones listed in Table 1 in Report II.

As a welding equipment, a whole vacuum type electron beam welding machine 150KV-40mA (6KW) of high voltage type (Hamilton type) was used. For welding method, as conducted a bead-on-plate test by flat welding method for partial penetration welding with weld bead put on materials used. Table 1 shows the welding conditions adopted.

Table 1 Welding conditions in this experiment.

Conditions / Materials	V_b (kv)	I_b (mA)	V_b (cpm)	D_F^* (mm)	θ_s (°)	Pch (Torr)	X-deflection Ax (mm)	Y-deflection Ay (mm)	Deflection frequency, Af (Hz)
SUS304	150	30	30,60	280	0	4×10^{-4}	0 - 1	0 - 1	0 - 1000
SUS304N	〃	〃	60	〃	〃	〃	〃	〃	〃
SM41	〃	〃	〃	〃	〃	〃	—	—	—
1200	〃	〃	〃	〃	〃	〃	0 - 2	0 - 2	0 - 5000
5083	〃	〃	60-240	〃	〃	〃	0 - 2	0 - 2	0 - 5000

2.2 Photographing method of X-ray characteristics occurring from beam holes in molten pool

We photographed X-ray occurring from beam hole during welding on a film, and studied on the relationship between the penetration depth or the shape of spikes and the concentration of X-ray. Fig.1 shows schematic diagram of used lead pinhole camera. A welding

† Received on July 28, 1975

* Professor

** Kawasaki Heavy Industries, Ltd.

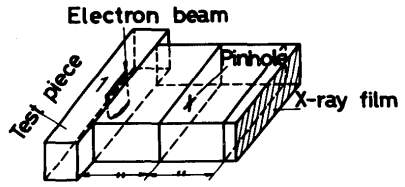

Fig. 1 Schematic representation of pin-hole camera used.

specimen was set on the left, X-ray film at the right end, and 3mm thick lead plate was put at the center of the above two. A 1mm pin-hole was made at the center of this lead plate and X-ray amount occurring from welding specimen side and also from the lower part was made sensitized on a film. As for industrious film, Fuji 50, Fuji 150 and Pb fluorescence screen were used.

After welding, the existence of porosity was checked by radiographic inspection from a side of welding specimen. Then a longitudinal section was planed and penetration depth and solidification pattern were observed.

2.3 Observation method of solidification pattern by using insert metal

For observing the movement of weld metal during welding, a welding specimen with insert metals inserted from the side with constant spacing was made following the instructions shown in Fig.2. Welding was conducted

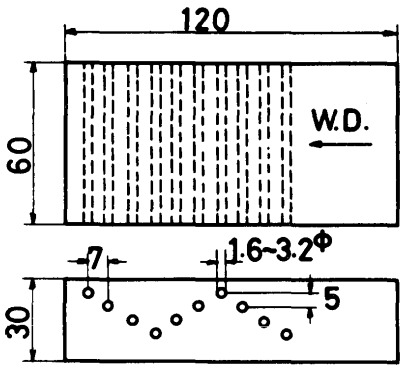

Fig. 2 Configration of weld specimen.

after grease was removed. For insert metals, covered electrode core wire (SWRY-11,2.6ϕ), covered electrode core wire for cast iron (DFC.Ni, 3.2ϕ), silver brazing filler metal (BAg-2, 35Ag-26Cu-21Zn-18Cd, 1.6ϕ), brass brazing filler metal (BCuZn-3,58Cu-42Zn, 2.0ϕ) and alminium electrode wire (A1200-BY, 2.4ϕ) were used.

After the welding, transverse section and longitudinal section at the center of each bead were planed out, and then the relationship between weld solidification pattern which insert metal occurred as segragation and weld defect was observed. Also spot analysis was conducted by an electron probe micro analyser (E.P.M.A.) for checking segregation of insert material. Etching reagents used for observation of solidification pattern are listed below.

10%$C_2H_2O_4$ (electrolytic etching) for SUS 304, SUS304N

20%$HC1O_4$ (electrolytic polishing) for 1200, 5083

5%HF acqueous solution (etching)

3. Experimental results

3.1 Observation of penetration phenomenon by X-ray occurring from beam hole inside molten pool

(a) Difference of X-ray characteristics by materials

As for SUS304, 1200 and 5083 alloys, a X-ray film (side film) photographed X-ray occurring from beam hole during welding with constant welding condition like a_b*=0.75 by a pin-hole camera set on the side of the specimen and a radiograph (side photograph) taken from the side were compared. Photo. 1 shows the compared photographs. As a result, it seems that the concentration is richer at the part where A-porosity occurs compared

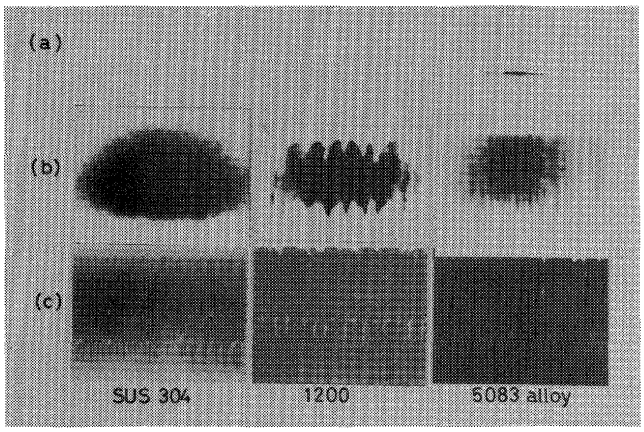

Photo.1 X-ray film photographed from side and back side of weld bead by pin-hole camera and raidography.
(a) X-ray film from back side of weld bead.
(b) X-ray film from side of weld bead.
(c) Radiograph of weld bead.

to the other parts, but in general, the concentration distribution is comparatively uniform, and the beam movement inside beam hole seems to be comparatively stable compared to the case with aluminium alloy.

On the other hand, in case with 1200 and 5083 alloys, periodical light and shade phenomenon was seen and the light and shade shape at the root part was perfectly in accordance with the occurring position of strong spikes. Also on the film (back side film) photographed from the bottom side of weld specimen, dots like spots tied in a row were recognized, which was different from the case of SUS304 with indefinite light

and shade phenomenon.

Form such observation results, it became clear that formation of needle spike or porosity strongly depend upon periodical change of beam flow strength inside beam hole. And it was recognized that formation of needle spike or porosity were also affected not only by weld condition but also by material.

(b) Influence of deflected beam

As for SUS304, 1200 and 5083 alloys, X-ray film and radiograph (side photograph) photographed X-ray amount occurring during welding using stationary beam and deflected beam were compared. Photos. 2,3 and 4 show the results of the abovementioned comparison

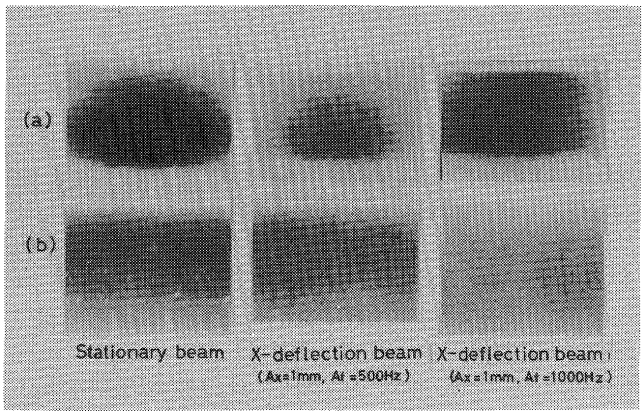

Photo.2 X-ray film photographed from side of weld bead by pin-hole camera and radiography (SUS304).
(a) X-ray film (b) Radiograph

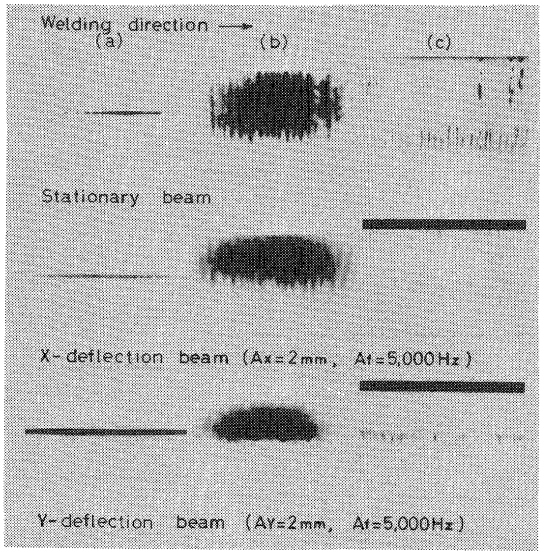

Photo.3 X-ray film photographed from side of weld bead by pin-hole camera and radiography (1200).
(a) X-ray film (b) Radiograph
(c) Macrostructure

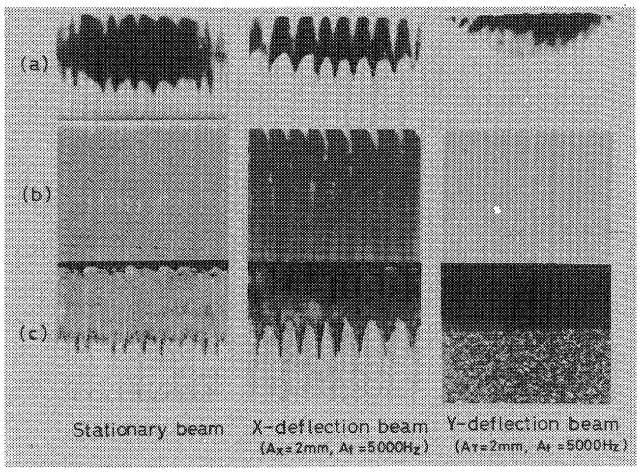

Photo.4 X-ray film photographed from side and back side of weld bead by pin-hole camera and raidography (5083 alloy).
(a) X-ray film from back side of weld bead.
(b) X-ray film from side of weld bead.
(c) Raidograph of weld bead.

with SUS304, the concentration at the part where A-porosity occurred seemed to be darker than the one at the other part on X-ray film photographed from the side in A-porosity occurring weld condition (stationary beam). Also in the A-porosity not occurring condition (X-deflection beam), very uniform concentration distribution was indicated.

In case of 1200 and 5083 alloys with the weld condition where AR porosity easily occurred (stationary beam), periodical light and shade of X-ray amount was shown on the side film, which was complately in accordance with strong spike position. Then in welding with X-deflection beam with 2mm amplitude, occurring frequency of AR-porosity became much higher than the one in case of stationary beam, and the spike forms became much sharper needle forms (needle spike). Also on the side film, light and shade degree became much stronger correlatively. Also on the back side film, dark dots were recognized tied in a row like spots marks which were much larger than the ones seen in case of stationary beam.

On the other hand, in case with welding in Y-deflection beam with 2mm amplitude, AR-porosity disappeared, and correlatively, periodical light and shade on the side film also disappeared. And uniform concentration distribution of X-ray amount was shown. Also on the back side film, a line was observed and no dots were recognized.

(c) Influence of a_b* value and welding speed

Photo. 5 shows the results of observing the side film, the side photograph and macrostructure of longitudinal section in case of changing a_b* value using 1200. In welding with beam active zone (a_b* $\fallingdotseq$ 0.75),

AR-porosity occurred, and needle spike was formed.

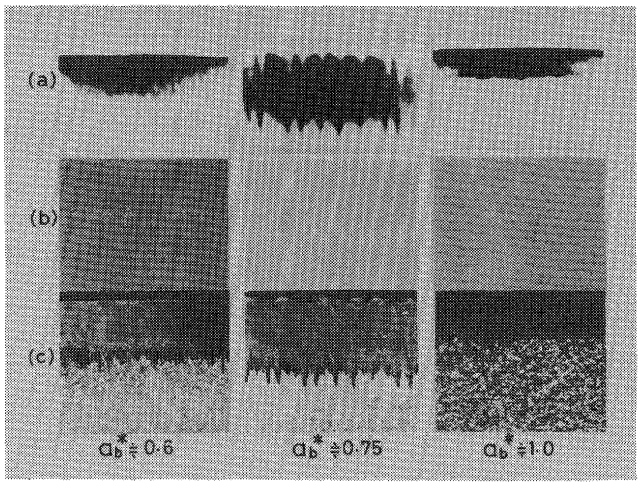

Photo. 5 X-ray film photographed from side of weld bead by pin-hole camera and radiography (1200).
(a) X-ray film (b) Radiograph
(c) Macrostructure

In this case, periodical strong light and shade appeared on the side film. In beam convergen zone ($a_b^* = 0.60$), periodical light and shade appeared also. But its degree became very weak, and correlatively spike forms became weak, too. Also a beam divergent zone ($a_b^* \fallingdotseq 1.0$), no periodical light and shade appeared at all, and neither AR-nor R-porosity occurred.

Next, Photo. 6 shows the result when welding speed was changed using 5083 alloy. In the range of the weld speed 60 ~ 240cm/min., the degree of light and shade appearing on the film became weak as the speed increased.

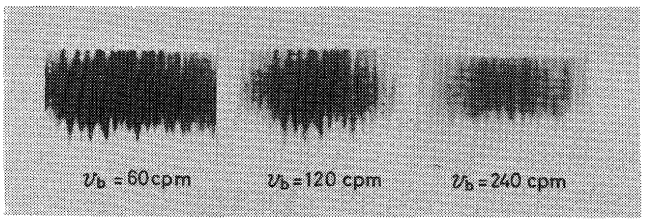

Photo. 6 X-ray film photographed from side of weld bead by pin-hole camera (5083 alloy).

But in this case, periodical light and shade was recognized clear even when penetration depth became most slight as V_b = 240cm/min. This shows that electron beam flow flowing into weld line per unit length became little and film density of X-ray became small when welding speed increased, but its periodical change was roughly constant not depanding upon welding speed. The periodical change of light and shade in this case is equivalent to approximately 1.7×10^{-1} sec/cycle. It can be considered that such periodicity is caused by strength if beam flow occurred inside beam hole, and this is closely related to the movement of weld metal of which will be mentioned below.

3.2 Observation of the movement of molten metal by using insert metal

(a) Observation of molten metal flow

Photo. 7 shows how the solidification pattern changes with a_b^* value a parameter using a specimen with mild steel rod inserted with making SUS304 base

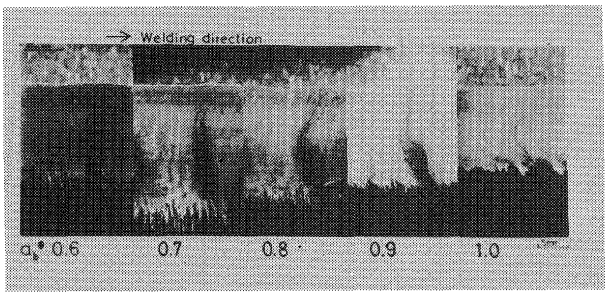

Photo. 7 Changes of solidification pattern on various a_b^* value in SUS304 welds. (Used covered electrode core wire for insert metal)

metals. In this photo., the change of solidification pattern formed by segregation of insert metal is shown clear.

When beam active zone is located near specimen surface ($a_b^* \fallingdotseq 0.70$), the segregation zone formed at the obliquely upper part of bead swollen part shows roughly vertical solidification pattern toward the root part from midway. Photo. 8 shows the micro structure of this part. It can be presumed easily that the molten metal of this

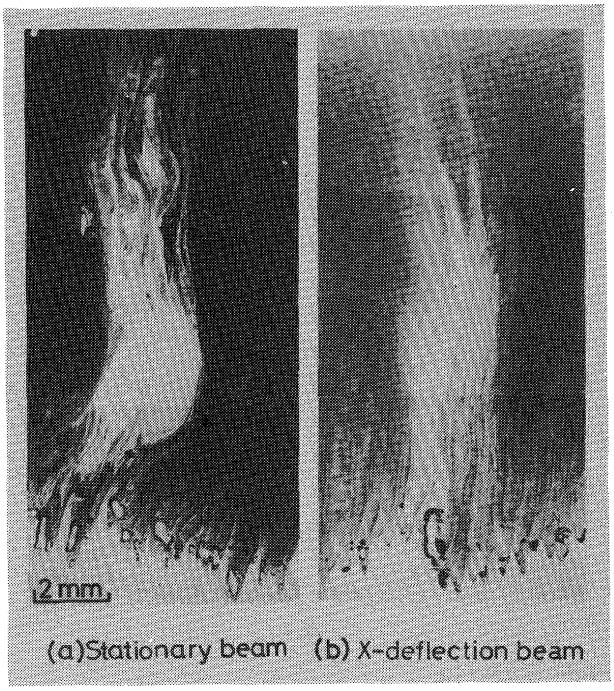

Photo. 8 Solidification pattern of longitudinal section of SUS304 welds.(Used covered electrode core wire for insert metal)

part show complicated fluidity because small spiral-formed pattern are seen here and there.

In welding in beam divergent zone ($a_b^* > 0.70$), typical arch type solidification pattern in the direction opposite to welding direction appeared. And spike strength gradually weakened and porosity gradually disappeared, too.

On the other hand, even in case with SUS304N with which A- and R-porosities easily occurred, solidification pattern nearly equivalent to the one with SUS304 was shown. Thus it is recognized that alloy component greatly affect on occurrence of porosity.

Fig. 3 shows the results of spot analysis test conducted by E.P.M.A. about segregation amount of molten insert metal. As the result, for both kinds of alloys, the segregation of insert metal became largest at $a_b^* = 0.7 \sim 0.8$ when A-porosity easily occurred, and after that, the segregation of insert metal decreased and showed alloying as a_b^* increased or decreased. This fact was caused by thermal conductivity of the alloy element accompanied with rapidly solidification and the difference of self diffusion. It can be considered that this fact had important relation with formations of "Wet beam hole" or "Dry beam hole", and also with occurring mechanism of porosity.

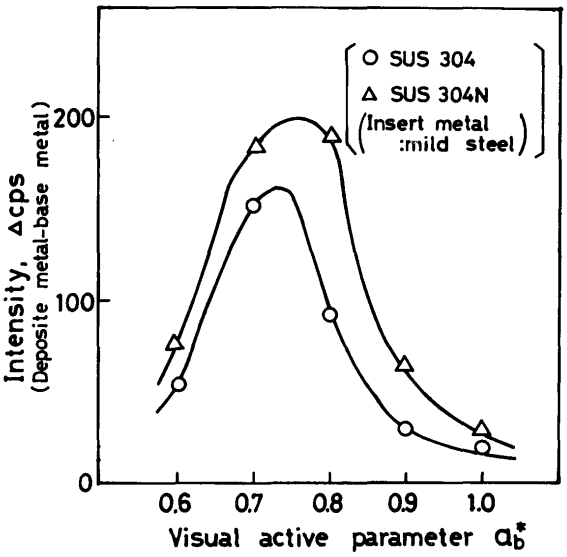

Fig. 3 Results of E.P.M.A. in stainless steel welds.

Next, Photo. 9 shows the result of the case welded by using stationary beam and X-deflection beam. The solidification pattern forming roughly vertical segregation band toward root part from the midway at the bead swollen zone in case of X-deflection beam was approximately equivalent to the one seen in case of stationary beam. But by observation of micro-structure, no small spiral-formed pattern appeared, and ripple line by columnar structure formed very regularly here as seen in Photo. 8. Also the size of crater in case of X-deflection beam became much bigger compared to the ones in case of stationary beam. In such solidification pattern, occurrence of porosity decreased clearly.

Photo. 10 shows the results of the case of aluminium alloy using brass brazing as insert metal. In

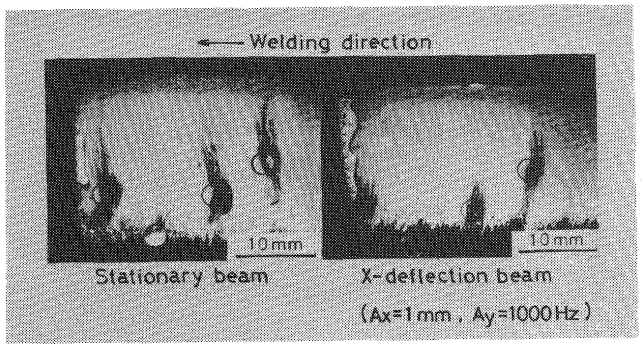

Photo. 9 Solidification pattern and crater pattern in longitudinal section in SUS304 welds. (Used covered ele ctrode core wire for insert metal)

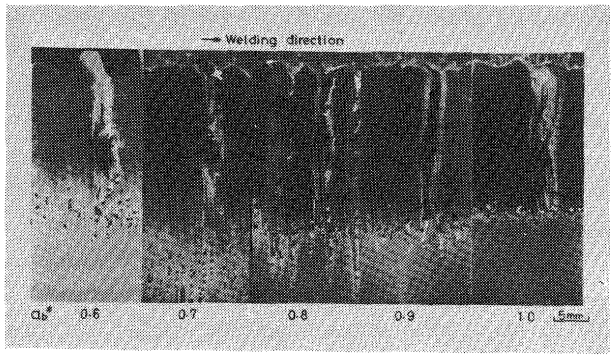

Photo. 10 Changes of solidification pattern on various a_b^* value in 1200 welds. (Used brass brazing filler metal for insert metal).

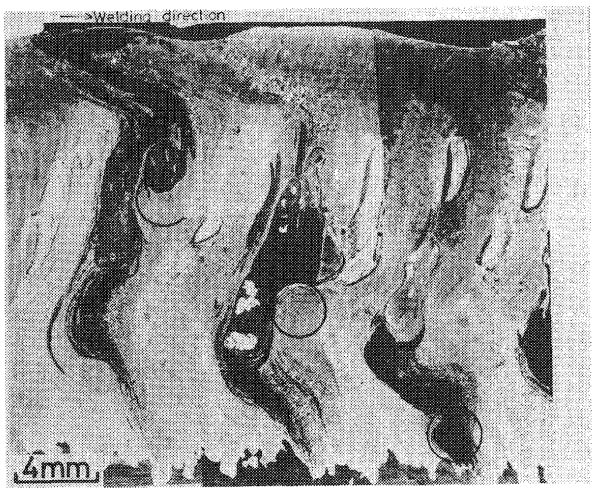

Photo. 11 Solidification pattern of segregation region in longitudinal section of SUS304N welds. (Used aluminum brazing filler metal for insert metal)

welding condition ($a_b^* \simeq 0.70$) in which AR-porosity and strong needle spike occurred, the solidification pattern formed, different from the one in case of iron-based alloy, a roughly vertical segregation band from the bead swollen part to the root part. But in a condition in which spike was very weak ($a_b^* \simeq 1.5$), the solidification pattern showed arch type which was equivalent to the one in case of iron-based alloy.

(b) Observation of occurring appearance of weld defect

Photo. 11 shows the solidification pattern of longitudinal section of specimen inserted pure aluminium into SUS304N as insert metal. As seen in this photograph, A-porosity occurred from irregularity point shown in segregation zone from obliquely upper part of the bead swollen zone down to the irregularity point near the root part.

The side radiograph and the longitudinal section solidification pattern of a specimen inserted silver brazing filler metal into SUS304 as insert metal were compared. Photo. 12 shows its compared results. At the position where insert metal was inserted, intermediate

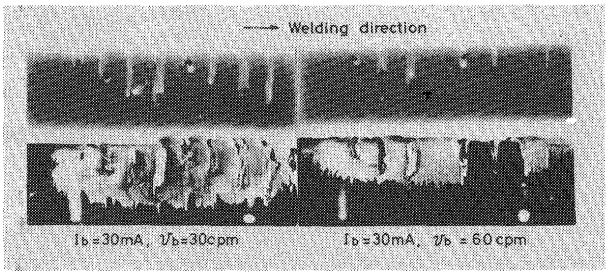

Photo. 12 Radiograph and macrostructure in SUS304 welds. (Used silver brazing filler metal for insert metal)
(a) Radiograph of weld bead (b) Macrostructure

defect between A-porosity and AR-porosity were recognized. It can be presumed that this defect occurred because very high inner pressure was generated inside beam by metal vapor generated with high vapor pressure elements like Cd and Zn silver brazing filler.

Also Photo. 13 shows the result of the case when silver brazing filler was inserted into 5083 alloy as insert metal. Normally, even in the condition when AR-

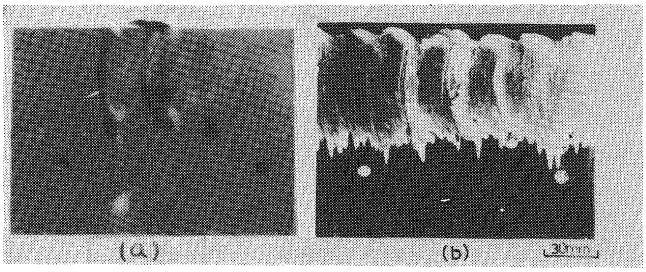

Photo. 13 Radiograph and macrostructure in 5083 alloy welds. (Used silver brazing filler metal for insert metal)
(a) Radiograph of weld bead (b) Macrostructure

porosity didn't occur, sometimes AR-porosity occurred. This shows that the influence of high vapor pressure element is so great.

4. Discussion

4.1 Behaviour of molten metal in molten pool

The penetration phenomenon was observed by X-ray occurred from beam hole in molten pool during electron beam welding. From the results of this observation, it became clear that X-ray characteristics of the case of iron-based alloy differ from a case of aluminium alloy. Also molten phenomenon was observed by conducting observation of segregation zone by insert metal. From these results, fluidities in molten pools of iron-based alloy and of aluminium could be presumed as below.

In other words, Fig. 4 (a) and (b) show the case with iron-based alloy in welding in beam active zone. In the figure (a), molten metal near the surface was apt to stop up the hole by tare weight of molten metal, and the upper part of hole became very narrow. Therefore it became difficult to discharge vapor metal or gas put inside. But as the figure (b) shows, the molten metal was pushed upward by the pressure because of the vapor pressure formed inside by the beam flow from the narrowed hole. At this time, a small swollen up hills made by molten metal were formed and therefore beam holes were pushed wide. At this time, the beam flow became to be concentrated to the bottom of root part, and spike occurred. Then molten metal was pushed out from the lower part to the upper part, and the condition was changed back to the (a) condition and the beam holes were apt to be stopped up. Thus the molten metal in molten pool was considered to move around.
molten pool was considered to move around.

In this case, the movement of molten metal at the beam active zone $a_b^* \doteqdot 0.75$ shows the spiral flow as the metal flows from the upper part and also from the lower part dashed against each other between the irregularity points B_1 and B_2 shown in the figure. Also the beam flow beyond B_1 point flows into molten pool in uniform, but the beam flow below B_1 point forms uniform beam flow.

Next, in case of aluminium alloy using the same beam condition as the above, the cooling rate was large and vapor pressure was high as aluminium alloy had stronger boiling phenomenon and larger thermal conductivity than iron-based alloy does. So in general, the molten metal around beam hole becomes less than the one in case of iron-based alloy, and molten metal us seemed to move upward straight along beam hole. Therefore no irregularity points exist inside a molten

pool as seen in case of iron-based alloy.

In beam divergent zone, neither iron-based alloy nor aluminium alloy shows strong molten metal movement as mentioned above. As Fig. 4(c) shows, the flow is stable.

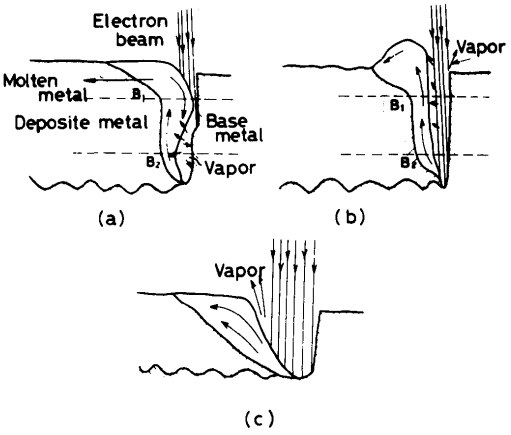

Fig. 4 Schematic illustration for behaviour of molten metal in welds.

4.2 Discussion on occurring condition of weld defect

In the previous item, the metal flow in molten pool during electron beam welding of iron-based alloy and aluminium alloy was described. At B_1 and B_2 irregularity points, though the positions were changed by electron beam conditions, the solidification line between B_1 and B_2 became very complicated as metal flows were dashed against each other from both upper and lower directions, and also the solidification became most slow here compared to the surface part and the root part. Therefore, it can be considered that voids occur easily here.

By the above discussion, occurrence of A-porosity of iron-based alloy is greatly caused by the fact that iron-based alloy had the irregularity points caused observing molten solidification process. For instance, the formation of these irregularity points can be prevented by A.C. deflection beam.

As shown in Photos. 12 and 13, it is recognized that AR-porosity occurs even in iron-based alloy not restrictly in aluminium alloy if high vapor pressure element like Cd or Zn exist in base metal. Moreover in this case, it was made clear that vaporization and spraying occur very heavily.

R-porosity occurs with strong spike when solidification line rises vertically up against the root part, but when the solidification line inclines, it decreases as spike is weakened. This phenomenon is equally seen either in iron-based alloy or in aluminium alloy.

As explained in Fig. 4, it can be considered that spiking occurs as beam energy reaching to the root part changes to act molten metal and beam flow each other as beam hole opens or closes periodically. In case of aluminium alloy, vaporization occurred violently, therefore vapor pressure in molten pool was higherthan iron-based alloy. Also the percentage of the beam flow to reach to the root part became large since thermal conductivity was large and molten metal was little. So strong spiking occurred. Thus it is important to consider occurrence of apiking based on the hole size and its amoount of surrounding molten metal. Photo. 14 shows typical example of "Wet beam hole" and "Dry beam hole". The whole penetration zone except the root part is "Wet beam hole" and the top part of the root is "Dry beam hole". Solidification rate is very large since no heat-affected zone was recognized, ferrite was not molten and only pearlite was changed.

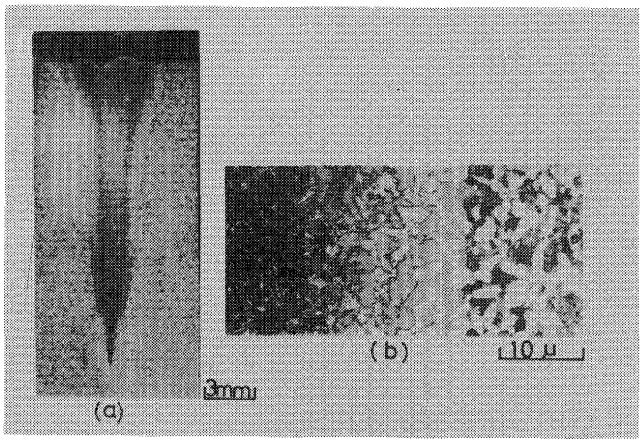

Photo. 14 Macro- and microstructure in cross section of SM41 welds.
(a) Macrostructure (b) Microstructure

5. Conclusion

We studied on the relationship between weld phenomenon and weld defect by investigating distribution characteristics of X-ray amount occurring from beam hole during electron beam welding and by observing solidification pattern of welding using insert metal.

1) Penetration phenomenon was observed by X-ray occurre from beam hole in molten pool. As the result, it becomes clear that X-ray characteristics differ from iron-based alloy to aluminium.

2) It was recognized that X-ray amount occurring from beam hole changed periodically in aluminium alloy, and this phenomenon was completely in accordance with spiking. And the cycle of this periodical change was roughly constant not depending on either a_b* value or welding speed so much.

3) The changes of solidification pattern formed by segregation using specimen inserted the insert metal was observed. As the result, it is considered voids are easily formed in case of iron-based alloy since molten metal flow moves complicatedly at irregularity points formed in molten pool in beam active zone. In beam divergent zone, typical arch type solidification pattern was shown in both cases of iron-based alloy and of aluminium alloy.

4) It was made sure that AR-porosity occurs even in iron-based alloy if high vapor pressure element like Cd or Zn exists in base metal.

5) The penetration phenomenon by X-ray occurring from beam hole in molten pool and the movement of molten metal using insert metal were observed. As the result, it can be concluded that the movement of metal flow in molten pool and the changes of beam flow are closely related and therefore defect is formed by the interaction among them.

References

1) Y. Arata, K. Terai, S. Matsuda: "Study on Characteristics of Weld Defect and Its Prevention in Electron Beam Welding (Report I). " Trans. of JWRI, Vol. 2, No. 1 (1973); IIW Doc. IV-112-73.

2) Y. Arata, K. Terai, S. Matsuda: "Study on Characteristics of Weld Defect and Its Prevention in Electron Beam Welding (Report II)." Trans, of JWRI, Vol. 3,No. 1 (1974), IIW Doc. IV-147-74.

3) Y. Arata, K. Terai, S. Matsuda: "Study on Characteristics of Weld Defect and Its Prevention in Electron Beam Welding (Report III)." Trans. of JWRI, Vol. 3, No. 2 (1974).

4) Y. Arata: "Super High Energy Density Beam Heat Source and Its Application." Kinzoku Hyomen Gijutsu, Vol. 24, No. 2 (1973).

5) Y. Arata, F. Matsuda, T. Murakami: "Some Dynamic Aspects of Weld molten metal in Electron Beam Welding." Trans of JWRI, Vol. 2, No. 2 (1973).